Volume 257, number 2, 403–407 FEB 07792 November 1989

A theoretical study of the acidification of the rhinovirus capsid

J. Warwicker

Department of Molecular Biophysics and Biochemistry and the Howard Hughes Medical Institute, Yale University, New Haven, CT 06511, USA

Received 13 July 1989; revised version received 18 September 1989

Electrostatic calculations for human rhinovirus 14 indicate that histidine-base residue pairs in the region of a β-strand interaction between pentamers may be involved in a pH-induced process that leads to the release of viral RNA. Other picornavirus sequences are examined for these residue pairs, a subset of which is present in enteroviruses. Foot and mouth disease virus possesses one of the residue pairs, and cardioviruses, which undergo a separate pH and halide ion-induced capsid dissociation, possess none.

Viral uncoating; Electrostatic modeling; pH dependence; Picornavirus; Histidine residue

1. INTRODUCTION

Picornaviruses are a large family of small animal viruses that contain single-stranded RNA. They are grouped into four genera [1,2]: enteroviruses (e.g. polio and coxsackie viruses), cardioviruses (e.g. encephalomyocarditis and Mengo viruses), rhinoviruses, and aphtoviruses (e.g. foot and mouth disease virus). Picornaviruses are assigned to these genera on the basis of physical properties such as buoyant density, pH lability of infectivity and sedimentation coefficients. The pH dependencies of infectivity vary substantially between the genera. Enteroviruses and cardioviruses maintain infectivity at pH 7 and at pH 4. However, cardioviruses lose infectivity in the presence of halide ions at slightly acidic pH (Mengo virus in 0.1 M halide ions at pH 6.3 [3], mouse Elberfeld (ME) virus in 0.1 M halide ions at pH 5.7 [4], and encephalomyocarditis virus (EMCV) in 0.1 M halide ions at pH 5.7 [5]). Aphtoviruses lose infectivity and are disrupted below pH 6.5, except at high ionic strength [6]. Rhinoviruses occupy an intermediate position, being disrupted below pH 5.

Biochemical studies have shown that foot and mouth disease virus (FMDV) capsid, upon inactivation of the virus at pH 6.5, breaks into subunits that correspond to pentamers [6]. Pentamers are also thought to be the disruption products for Mengo virus [7], ME virus [4], and EMCV [5], in 0.1 M halide at pH 5.7. Acidification of rhinovirus to inactivate causes a conformational change in the capsid giving rise to a capsid particle with a much lower isoelectric point than that of the infectious particle [8]. Poliovirus, without being inactivated, shows 2 isoelectric points [9], which are close to those of rhinovirus. Infectious Mengo virus can also exist in separate p*I* forms [10]. There is evidence that the observed acidic pH inactivations of picornaviruses are relevant to the cellular processes that cause release of the viral RNA. Endosomes and lysosomes have been implicated in the uncoating process [11,12].

Picornavirus structures have been solved at atomic resolution for one member of each of the genera; human rhinovirus 14 (HRV 14) [13], Mahoney strain poliovirus (an enterovirus) [14], Mengo virus (a cardiovirus) [15], and FMDV, an aphtovirus [16]. The 3-dimensional coordinates of HRV 14 and of Mengo virus are in the protein data bank (PDB) [17] of 1988. The capsid of each picornavirus is organised as an eicosahedral particle with 60 protomers, arranged in 12 pentamers. Each protomer has one copy of 4 viral coat proteins, VP1, VP2, VP3 and VP4.

Electrostatic interactions play a major role in the energetics of macromolecular systems. In particular, they mediate pH-dependent phenomena. Computational techniques to calculate electrostatic interactions have been successful in accounting qualitatively for pH-dependent phenomena such as ligand binding and the protonation state of active site residues [18]. The study reported here uses electrostatic calculations to predict regions in the HRV 14 capsid that may cause conformational changes upon acidification. The electrostatic calculations are more suited to modelling effects that are pH-dependent alone (HRV), without additional ion-induced effects (Mengo virus). Most of the article is therefore devoted to modelling the HRV acidification. Some calculations on Mengo virus are discussed. The calculations presented in this article do not address the considerable problem of accounting for

Correspondence (present) address: J. Warwicker, AFRC Institute of Food Research, Reading Laboratory, Shinfield, Reading RG2 9AT, England

Published by Elsevier Science Publishers B.V. (Biomedical Division)

the very large p*I* changes observed for some picornaviruses.

2. MATERIALS AND METHODS

The PDB coordinate set 2RHV has been used. Calculations of electrostatic energies as a function of pH were performed with a charge-charge interaction formula that has been described previously [19,20]. An effective dielectric value of 50 and a Debye-Huckel factor at an ionic strength of 0.1 M have been used. The side chain charges of ionisable amino acids and charges representing the macro-dipole of the α-helix (a half unit charge at either end of the helix), were included. These calculations give an electrostatic energy for each ionisable residue interacting with the other charges in the system, at a single pH. The difference between electrostatic energies at separate pH values, for each ionisable residue, is placed onto a 3-dimensional grid, contoured, and displayed graphically with the program FRODO [21] on an Evans and Sutherland colour graphics system.

3. RESULTS

Acidification of the native (crystal) HRV 14 structure at pH 5 causes loss of infectivity and a conformational change. The calculation strategy is therefore to look for regions in the native structure that are destabilised upon the pH 7 to pH 5 change. Since the native conformation alone is known, it is not possible to investigate the second part of the stability equation directly, i.e. stabilisation from pH 7 to 5 of the inactivated conformation. Stability changes will be centred on the ionisable residues that have p*K* values in this range. The p*K* of an acidic group (aspartic or glutamic acid) ionising between pH values 7 and 5 would be higher than the normal p*K* (without interactions with other charges). An increased p*K* for an acidic group implies an unfavourable interaction with neighbouring negative charge. The pH change from 7 to 5 increases the positive charge on the molecule, stabilising such an acidic group. An example of this effect has been postulated for tobacco mosaic virus (TMV) protein [22]. In TMV it appears that pairing of carboxylate groups, with p*K* values around neutral, in the virus but not in other protein aggregates leads to a relative stability of the virus aggregate at low pH [22]. It is expected that instability of a particular conformation over the pH 7 to 5 range will be generated by basic groups. Histidine residues in particular (with a normal p*K* of about 6.5), interacting unfavourably with neighbouring positive charge could have reduced p*K* values close to 5.

Fig.1 shows the negative electrostatic energy differences from pH 7 to pH 5 for the ionisable residues of a protomer of the HRV 14 capsid and a 10 Å border set of atoms around this protomer. The negative contours, representing destabilisation from pH 7 to pH 5, show the strongest presence in the canyon region and in the pentamer-pentamer interface. It can be seen that the contour peaks normally appear as multiple clusters, often as 2 peaks. These arise from pairs of histidine residues and lysines or arginines, confirming the influence of the basic clusters on decreasing the histidine p*K* values.

Table 1 lists the 6 histidines that are destabilised most from pH 7 to pH 5, along with the bases that cause their changed p*K* values. They all have low solvent accessibility values. The development of a positive charge might, therefore, be expected to lead to a relatively unstable histidine environment, and possibly a conformational change with the histidine seeking to solvate its positive charge. The overall homology between aligned

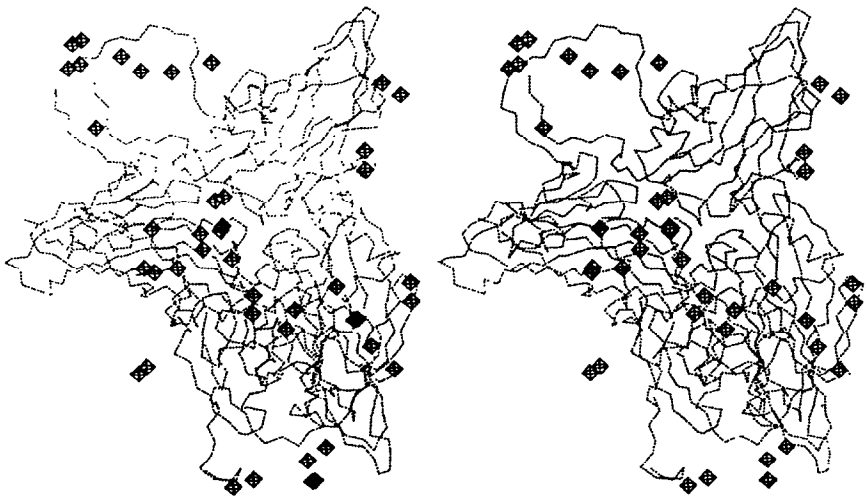

Fig.1. The α-carbon backbone of one HRV protomer (VP1, VP2, VP3 and VP4) is drawn in dotted lines. Contours of the difference in electrostatic energy between pH 7 and pH 5 for this protomer and a 10 Å border atom set are drawn as diamond shapes for the negative level at 0.75 kT (less stable at pH 5). The view is onto the outside of the capsid, with the normal to the capsid surface perpendicular to the figure. A pentamer is formed from protomers related to that drawn by a 5-fold axis on the left side of the figure. The edge running vertically on the right hand side of the figure takes part in a dimer interaction (with the dimer axis half way up this edge), that contributes substantially to pentamer-pentamer interactions. The path of the topological canyon feature [13] encircling the 5-fold axis is evident in the figure.

Table 1

Histidine-partner base pairs in HRV 14

Histidine	Location	SA (Å^2)	Partner		HRV2	Pol	Cox	FMDV	Mengo	TMEV	EMCV
VP1 27	pent.-pent.	0.5 (ND1)	dimer-rel	His	–	✓	–	*	*	*	*
	interface		K VP4 57	Base	✓	✓	✓	?	?	?	?
VP1 220	canyon	6.7 (NE2)		His	–	–	–	–	–	–	–
			K VP1 103	Base	–	–	–	–	–	–	–
VP1 245	canyon	0.4 (ND1)		His	✓	–	–	–	–	–	–
			K VP1 248	Base	✓	✓	✓	✓	✓	✓	✓
			H VP1 78	Base	✓	–	–	–	–	–	–
VP2 109	pent.-pent.	0.0	dimer-rel	His	✓	✓	✓	–	–	–	–
	interface		K VP3 126	Base	✓	✓	✓	R✓	✓	✓	✓
VP3 106	canyon	2.2 (NE2)		His	✓	✓	✓	–	–	–	–
			R VP3 220	Base	✓	✓	✓	✓	K✓	✓	K✓
VP3 150	pent.-pent.	0.0	dimer-rel	His	✓	✓	✓	✓	–	–	–
	interface		R VP2 62	Base	✓	✓	✓	✓	✓	✓	?

The solvent accessibilities [27] of the more accessible of the imidazole nitrogens are given. Sequence searches with other picornaviruses have been made with the PSQ match facility in the PIR database, and with a structural alignment of HRV 14, Mengo virus and FMDV [16]. A tick shows that the residue is present, a hyphen that the residue has changed, a question mark that the sequence homology is insufficient to match the sequence, and an asterisk that the polypeptide containing the residue is not present in the sequence being searched. Cox is Coxsackie virus, and Pol is polio virus

HRV 14 and HRV 2 sequences is 52% [23]. Histidine-partner base pairs that are present in HRV 14 and in HRV 2 are (VP1 245-VP1 78 and VP1 248) and (VP3 106-VP3 220) in the canyon and (VP2 109-dimer-related VP3 126) and (VP3 150-dimer-related VP2 62) in the pentamer-pentamer interface. Histidines VP2 109 and VP3 150 have zero solvent accessibility in the HRV 14 structure, suggesting that conformational changes in the pentamer-pentamer interface may play a role in the pH-induced conformational change, along with possibly canyon region changes around histidines VP1 245 and VP3 106. Fig.2 shows the part of the pentamer-pentamer interface of HRV 14 containing the 2 histidine-partner base pairs (VP2 109-VP3 126) and (VP3 150-VP2 62). This figure also shows the continuation of a β-sheet between the 2 pentamers in the same region, emphasising the possible relevance of these 2 histidine-partner base pairs to pentamer association.

Calculations of electrostatic complexation energies indicate that interactions within a pentamer become more stable from pH 7 to pH 5 (by about 21 kJ/mol per protomer), whilst pentamer-pentamer interactions

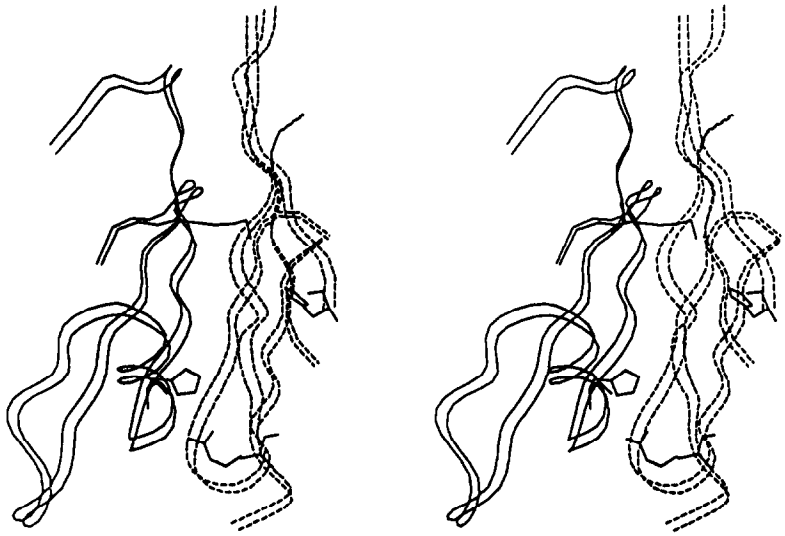

Fig.2. A stereo view of part of the pentamer-pentamer interface of HRV 14. Parts of strands βE1 and βF of VP3 [13], and the polypeptide between them are shown in solid ribbon. From another protomer in a neighbouring pentamer, parts of strands βA1, βA2, βB, βD and βI of VP2 are shown in dashed ribbon. Two histidine-partner base pairs are shown, each formed across the pentamer-pentamer interface. The lower one in the figure is His VP3 150-Arg VP2 62 and the upper one is His VP2 109-Lys VP3 126.

weaken over this pH range (by about 12 kJ/mol for each protomer-protomer interaction across the 2-fold axis). This weakening reflects the effect of the histidines in the pentamer-pentamer interfaces that exist in the crystal structure form of the capsid.

4. DISCUSSION

None of the histidine-partner base pairs listed in table 1 are present throughout the cardioviruses as pairs, which is consistent with the absence of a pH-induced conformational changes analogous to that of rhinoviruses in cardioviruses. One of these pairs, equivalent to VP3 150-VP2 62 in HRV 14, is present in FMDV. A high density of histidines have been reported in the pentamer-pentamer interface [16], which could be linked with the dissociation into pentamers at pH 6.5. It is possible that these histidines (including that equivalent to VP3 150 of HRV 14) play a similar role to those listed for HRV 14, but closer to neutral pH and the normal histidine pK. Such histidines should then interact less with neighbouring positive charge.

Three of the histidine-partner base pairs are present in the enteroviruses polio and coxsackie, including the 2 in the pentamer-pentamer interface shown in fig.2. In rhinoviruses, the results described in this article suggest that a subset of these 3 pairs and one more, in the canyon region, are responsible for a pH-induced conformational change in the capsid that leads to loss of viral RNA. Since enteroviruses are able to maintain infectivity over the pH range of the rhinovirus transition, any conformational change associated with the 3 common pairs cannot lead to the loss of viral RNA. Intact and infectious poliovirus can, however, exist in 2 reversible conformational forms, one favoured at neutral pH and the other at acidic pH [1,24]. It is possible that the histidine-partner base pairs that are predicted to provide a molecular basis for the pH-induced uncoating of rhinoviruses combine with one or more other effectors (such as other regions of conformational change in the capsid or receptor binding and cell entry), to promote RNA loss from enteroviruses. These predictions are consistent with observations of the low pH-induced infection of poliovirus bound to the cell surface [24].

The binding of a class of antiviral drugs to HRV 14 has been characterised biochemically and structurally [25,26]. It is proposed that the drugs, which bind in the hydrophobic interior of the VP1 β-barrel, prevent the conformational change in the capsid that leads to loss of viral RNA by making the capsid more rigid [26]. Of the 4 histidine-partner base pairs present in both HRV 14 and HRV 2, 2 are in the canyon region and 2 in the pentamer-pentamer interface. It seems likely that the sites of pH-induced change transmit conformational rearrangement to the whole capsid. Since 3 out of 4 of the sites predicted for rhinoviruses are present in enteroviruses, it may be that the analogous, but not RNA releasing change, in enteroviruses differs in part in the propagation of the changes through the capsid.

Calculations of pK values and probe accessibilities have been made for the histidine residues of Mengo virus, using the 1MEV PDB coordinate set. The sharp optimum of the dissociation into pentamers at pH 6.2 [3] suggests that a group with a pK of around 6.2, in the presence of halide ions, is involved. Several

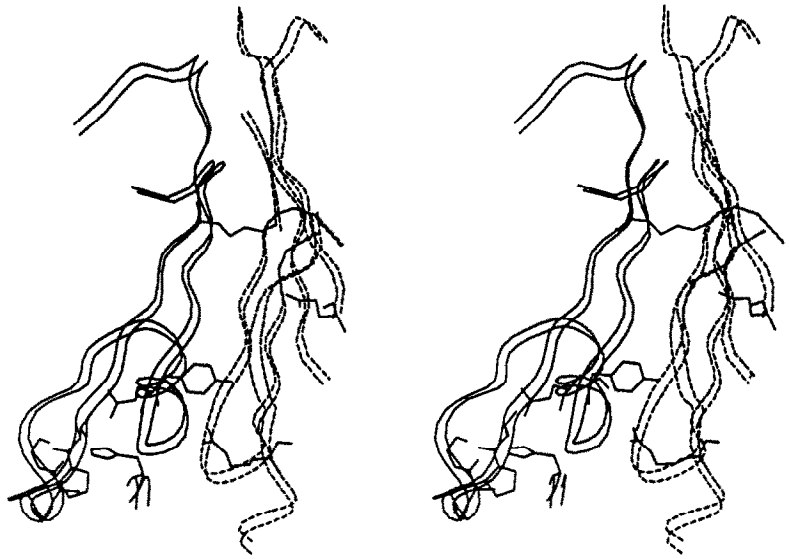

Fig.3. A stereo view of the part of the pentamer-pentamer interface for Mengo virus which is equivalent to that shown for HRV 14 in fig.2. The residue pairs Tyr VP3 147-Arg VP2 62 (lower) and Gln VP2 113-Lys VP3 123, that are structurally homologous to the histidine-partner base pairs of HRV 14, are shown. In the lower part of the figure, histidine 250 of VP2 is drawn, together with the sequential residues Thr-Pro-Pro-Gly-Ala-Gly (129–134) and Asn 141 from VP3 of the same protomer. Histidine VP2 250 of Mengo virus interacts with main-chain atoms of residues Ala VP3 133 and Gly VP3 134 and with side-chain atoms of Thr VP3 129, Ala VP3 133 and Asn VP3 141. The peptide link between Ala VP3 133 and Gly VP3 134 of Mengo virus is reversed from that in the equivalent loop in the HRV 14 structure.

histidines are calculated to have pK values close to 6.2. Of these, histidine 250 of VP2 shows additional interesting features. Its calculated accessibility to probes of varying radii falls to zero as the radius increases from chloride ion to iodide ion. Fig.3 shows that this histidine interacts with the loop sequence between the two VP3 β-strands that are structurally homologous to those in HRV 14 that each contribute a residue to the histidine-partner base interactions in the pentamer interface (shown in fig.2). These 2 pair histidines of HRV 14 have been replaced by Gln VP2 113 and Tyr VP3 147 of Mengo virus. In HRV 14 the residue equivalent to His VP2 250 of Mengo virus, Ser VP2 256, does not make such extensive interactions across the loop.

The histidine at position 250 of VP2 in Mengo virus and the Mengo virus loop sequence with which it interacts are present in the cardioviruses EMCV and Theiler's murine encephalomyelitis virus (TMEV). With a predicted pK of 6.2 and with part of its imidazole ring accessible to chloride ions, histidine VP2 250 of Mengo virus could change conformation under the dissociation conditions [3], and destabilise the native loop structure and the pentamer-pentamer interface. The Mengo virus dissociation has been investigated experimentally (Rossmann, M., personal communication) by soaking native Mengo virus crystals in halide ions at pH 6.2 for short periods of time. The resulting changes, whilst not sufficient to give large-scale crystal and capsid disruption, are taken to indicate the first steps of the dissociation. Histidine 250 of VP2 is not observed to change and is therefore not invoked in a capsid dissociation mechanism deduced from crystallographic analysis of the Mengo virus crystal soaks. However, since this experiment depends upon maintaining the crystal lattice which must eventually break in the dissociation process, it cannot rule out the involvement of conformational changes other than those observed (possibly including His VP2 250) in the capsid dissociation.

Acknowledgements: The author wishes to thank M. Rossmann for communicating results prior to publication, and for helpful discussions. R. Pickersgill is also thanked for providing discussion. F. Quiocho and P.R. Evans are thanked for supplying their versions of the program FRODO. The Howard Hughes Medical Institute and the AFRC are thanked for providing support during this work.

REFERENCES

[1] Koch, F. and Koch, G. (1985) in: The Molecular Biology of Poliovirus, Springer, Wien.
[2] Rueckert, R.R. (1976) in: Comprehensive Virology, vol.6, chapter 5 (Fraenkel-Conrat, H. and Wagner, R.R. eds) Plenum, New York.
[3] Mak, T.W., O'Callaghan, D.J. and Colter, J.S. (1970) Virology 40, 565–571.
[4] Dunker, A.K. and Rueckert, R.R. (1971) J. Mol. Biol. 58, 217–235.
[5] McGregor, S., Hall, L. and Rueckert, R.R. (1975) J. Virol. 15, 1107–1120.
[6] Talbot, P., Rowlands, D.J., Burroughs, J.N., Sangar, D.V. and Brown, F. (1973) J. Gen. Virol. 19, 369–380.
[7] Mak, T.W., Colter, J.S. and Scraba, D.G. (1974) Virology 57, 543–553.
[8] Korant, B.D., Lonberg-Holm, K., Yin, F.H. and Noble-Harvey, J. (1975) Virology 63, 384–394.
[9] Mandel, B. (1971) Virology 44, 554–568.
[10] Chlumecka, V., D'Obrenan, P. and Colter, J.S. (1977) J. Gen. Virol. 35, 425–437.
[11] Merion, M., Schlesinger, P., Brooks, R.M., Moehring, J.M., Moehring, T.J. and Sly, W.S. (1983) Proc. Natl. Acad. Sci. USA 80, 5315–5319.
[12] Zeichhardt, H., Wetz, K., Willingmann, P. and Habermehl, K.-O. (1985) J. Gen. Virol. 66, 483–492.
[13] Rossmann, M.G., Arnold, E., Erickson, J.W., Frankenberger, E.A., Griffith, J.P., Hecht, H.-J., Johnson, J.E., Kamer, G., Luo, M., Mosser, A.G., Rueckert, R.R., Sherry, B. and Vriend, G. (1985) Nature 317, 145–153.
[14] Hogle, J.M., Chow, M. and Filman, D.J. (1985) Science 229, 1358–1365.
[15] Luo, M., Vriend, G., Kamer, G., Minor, I., Arnold, E., Rossmann, M.G., Boege, U., Scraba, D.G., Duke, G.M. and Palmenberg, A.C. (1987) Science 235, 182–191.
[16] Acharya, R., Fry, E., Stuart, D., Fox, G., Rowlands, D. and Brown, F. (1989) Nature 337, 709–716.
[17] Bernstein, F.C., Koetzle, T.F., Williams, G.J.B., Meyer, E.F., jr, Brice, M.D., Rodgers, J.R., Kennard, O., Shimanouchi, T. and Tasumi, M. (1977) J. Mol. Biol. 112, 535–542.
[18] Matthew, J.B. (1985) Annu. Rev. Biophys. Chem. 14, 387–417.
[19] Warwicker, J., Ollis, D., Richards, F.M. and Steitz, T.A. (1985) J. Mol. Biol. 186, 645–649.
[20] Warwicker, J., Engelman, B.P. and Steitz, T.A. (1987) Proteins 2, 283–289.
[21] Jones, T.A. (1978) J. Appl. Crystallogr. 11, 268–272.
[22] Butler, P.J.G., Durham, A.C.H. and Klug, A. (1972) J. Mol. Biol. 72, 1–18.
[23] Blaas, D., Kuechler, E., Vriend, G., Arnold, E., Luo, M. and Rossmann, M.G. (1987) Proteins 2, 263–272.
[24] Olsnes, S., Madshus, I.H. and Sandvig, K. (1986) in: Virus Attachment and Entry into Cells (Crowell, R.L. and Lonberg-Holm, K. eds) pp.171–181, American Society for Microbiology, Washington, DC.
[25] Smith, T.J., Kremer, M.J., Luo, M., Vriend, G., Arnold, E., Kamer, G., Rossmann, M.G., McKinlay, M.A., Diana, G.D. and Otto, M.J. (1986) Science 233, 1286–1293.
[26] Badger, J., Minor, I., Kremer, M.J., Oliveira, M.A., Smith, T.J., Griffith, J.P., Guerin, D.M.A., Krishnaswamy, S., Luo, M., Rossmann, M.G., McKinlay, M.A., Diana, G.D., Dutko, F.J., Fancher, M., Rueckert, R.R. and Heinz, B.A. (1988) Proc. Natl. Acad. Sci. USA 85, 3304–3308.
[27] Lee, B. and Richards, F.M. (1971) J. Mol. Biol. 55, 379–400.